ARTICLES
PUBLISHED ONLINE: 21 SEPTEMBER 2015 | DOI: 10.1038/NNANO.2015.219
nature nanotechnology

Identification of single nucleotides in MoS_2 nanopores

Jiandong Feng[1†], Ke Liu[1†], Roman D. Bulushev[1], Sergey Khlybov[1], Dumitru Dumcenco[2], Andras Kis[2] and Aleksandra Radenovic[1*]

The size of the sensing region in solid-state nanopores is determined by the size of the pore and the thickness of the pore membrane, so ultrathin membranes such as graphene and single-layer molybdenum disulphide could potentially offer the necessary spatial resolution for nanopore DNA sequencing. However, the fast translocation speeds (3,000–50,000 nt ms^{-1}) of DNA molecules moving across such membranes limit their usability. Here, we show that a viscosity gradient system based on room-temperature ionic liquids can be used to control the dynamics of DNA translocation through MoS_2 nanopores. The approach can be used to statistically detect all four types of nucleotide, which are identified according to current signatures recorded during their transient residence in the narrow orifice of the atomically thin MoS_2 nanopore. Our technique, which exploits the high viscosity of room-temperature ionic liquids, provides optimal single nucleotide translocation speeds for DNA sequencing, while maintaining a signal-to-noise ratio higher than 10.

Single nucleotide identification[1,2] and DNA sequencing[3] have already been demonstrated with biological nanopores. However, the fragility of such pores, together with difficulties related to measuring their pA-range ionic currents and their dependence on biochemical reagents, means that solid-state nanopores remain an attractive alternative[4]. In contrast to biological pores, solid-state nanopores can operate in various liquid media and pH conditions, their production is scalable and compatible with nanofabrication techniques[5], and they do not require the excessive use of biochemical reagents. These advantages are expected to make solid-state nanopore sequencing cheaper than sequencing with biological pores.

The basic sensing principle in sold-state nanopores is the same as in biological pores. A DNA molecule is threaded through a nanometre-sized pore under an applied potential and, ideally, the sequence of nucleotides is read by monitoring small changes in the ionic current flowing through the pore that are caused by individual nucleotides temporarily residing within the pore[6]. However, solid-state nanopores also allow a transverse detection scheme, which is based on detecting changes in the electrical conductivity of a thin semiconducting channel[4].

In both biological and solid-state nanopores, achieving an optimal translocation speed remains a significant challenge[7]. The optimal speed for DNA sequencing is 1–50 nt ms^{-1} (ref. 8). In a nanopore sequencer based on biological pores, translocation speeds are currently too slow (on the order of 2.5–70 nt s^{-1}, ref. 8) and are also limited by their use of enzymes. Therefore, to achieve genome sequencing, thousands—or even millons—of biological pores need to be integrated into one sequencer. In solid-state nanopores, translocation speeds are on the order of 3,000–50,000 nt ms^{-1}, the large range being a result of factors such as the pore size (1.5–25 nm) and the applied potential (100–800 mV)[9]. These fast speeds limit the ability of solid-state nanopores to reach single-nucleotide resolution, and are a major obstacle to the use of solid-state nanopores in the sequencing of DNA.

Solid-state nanopores also face problems regarding their low ionic current signal-to-noise ratios and relatively large sensing regions. The size of the sensing length is dictated by the thickness of the pore membranes, typically 10–20 nm, which can accommodate 30–60 nucleotides at a time[9]. To provide the necessary spatial resolution, nanopores have been fabricated in graphene membranes[10–12], creating solid-state nanopores at the ultimate thickness limit. Nanopores realized in three-layer graphene structures, which have a thickness of 1 nm, should display higher signal-to-noise ratios than single-layer graphene nanopores[13,14]. The use of two-dimensional materials such as graphene is potentially of additional value because it allows DNA translocation to be detected using two synchronized signals: the ionic current through the nanopore and the electrical current across the pore. Our group has recently shown that a silicon nitride nanopore can be integrated with a graphene nanoribbon transistor, and the translocation of DNA can be simultaneously detected using ionic currents and electrical currents[4]. However, pristine graphene nanopores exhibit strong hydrophobic interactions with DNA[15], which limits their long-term use because of clogging, so surface functionalization of the graphene is required[16].

Other two-dimensional materials such as boron nitride (BN)[17] and molybdenum disulphide (MoS_2)[18] have been explored as alternatives to graphene, and advances in fabrication methods have allowed nanopores in ultrathin SiN_x (ref. 19) and HfO_2 (ref. 20) to be created. MoS_2 nanopores are of particular interest as they can be used for extended periods of time (hours, and even days) without the need for any additional functionalization[18]. The sticking of DNA to MoS_2 nanopores is reduced by the Mo-rich region around the drilled pore after irradiation with a transmission electron microcope (TEM)[21], and their stability can be attributed to their relative thickness (single-layer MoS_2 has a thickness of 0.7 nm). Single-layer MoS_2 also has a direct bandgap of at least 1.8 eV (refs 4, 22), a feature that is essential for electronic base detection with field-effect transistors (FETs)[4,23]. Therefore, MoS_2 is a promising material for single-nucleotide detection, as was recently computationally demonstrated by Farimani and co-authors[24].

[1]Laboratory of Nanoscale Biology, Institute of Bioengineering, School of Engineering, EPFL, Lausanne 1015, Switzerland. [2]Laboratory of Nanoscale Electronics and Structure, Institute of Electrical Engineering, School of Engineering, EPFL, Lausanne 1015, Switzerland. †These authors contributed equally to this work. *e-mail: aleksandra.radenovic@epfl.ch

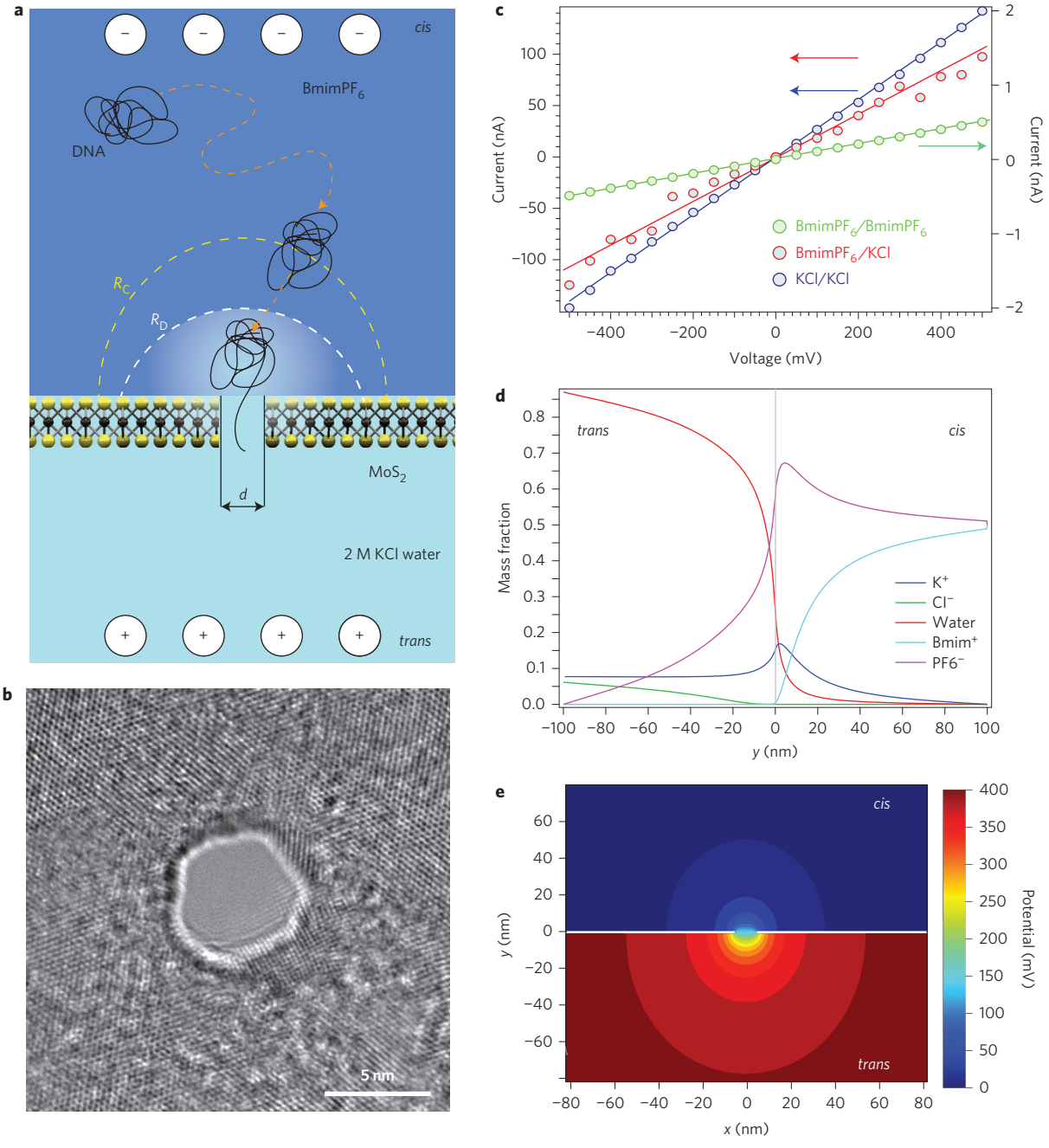

Figure 1 | Schematic and characterization of the RTILs/KCl viscosity gradient system in MoS_2 nanopores. a, The *cis* chamber contains RTILs ($BmimPF_6$) and the *trans* chamber contains 2 M aqueous KCl solution. The two chambers are separated by a monolayer MoS_2 membrane with a nanopore. The schematic also shows the dynamics of DNA translocation through a nanopore. Away from the pore, DNA motion is purely diffusive due to the negligible electric field, but once within the area of the capture radius R_c, DNA will be accelerated towards the pore by a force due to electrophoretic and electroosmotic effects. Part of the DNA will undergo conformational change and one end will dive into the pore. The non-translocated part of the DNA polymer-monomers will keep the coil conformation and experience a strong Stokes dragging force from the ionic liquids. Consequently, DNA translocation through the pore can be significantly slowed. **b**, Bright-field TEM image of a 5 nm solid-state pore fabricated in a monolayer MoS_2 membrane suspended over a 200 × 200 nm^2 etched area formed in the centre of a 20 μm low-stress SiN_x membrane with a thickness of 20 nm. **c**, Ohmic *I*–*V* responses of a 17 ± 2 nm MoS_2 pore. The *I*–*V* characteristics were taken at room temperature in a 2 M aqueous KCl solution (blue circles), pure $BmimPF_6$ (green circles) and in a $BmimPF_6$/2 M KCl gradient (red circles). **d**, Mass fraction of water, anions (PF_6^- and Cl^-) and cations ($Bmim^+$ and K^+) as a function of distance from the nanopore (note that the calculation was performed at −400 mV). **e**, Electric potential map evaluated numerically for the viscosity gradient system shown in **a**.

Viscosity gradient system in MoS_2 nanopores

A combination of atomically thin MoS_2 nanopores and an ionic liquid/water viscosity gradient system was used to decrease the molecular translocation speeds by two to three orders of magnitude. This approach to slowing down translocation was inspired by the remarkable physical and chemical properties of room-temperature ionic liquids (RTILs)—non-aqueous electrolytes composed of a pair of organic cations and anions. RTILs offer a high degree of freedom in fine-tuning their structure, which allows their physical and chemical properties to be tailored to a given application[25]. We

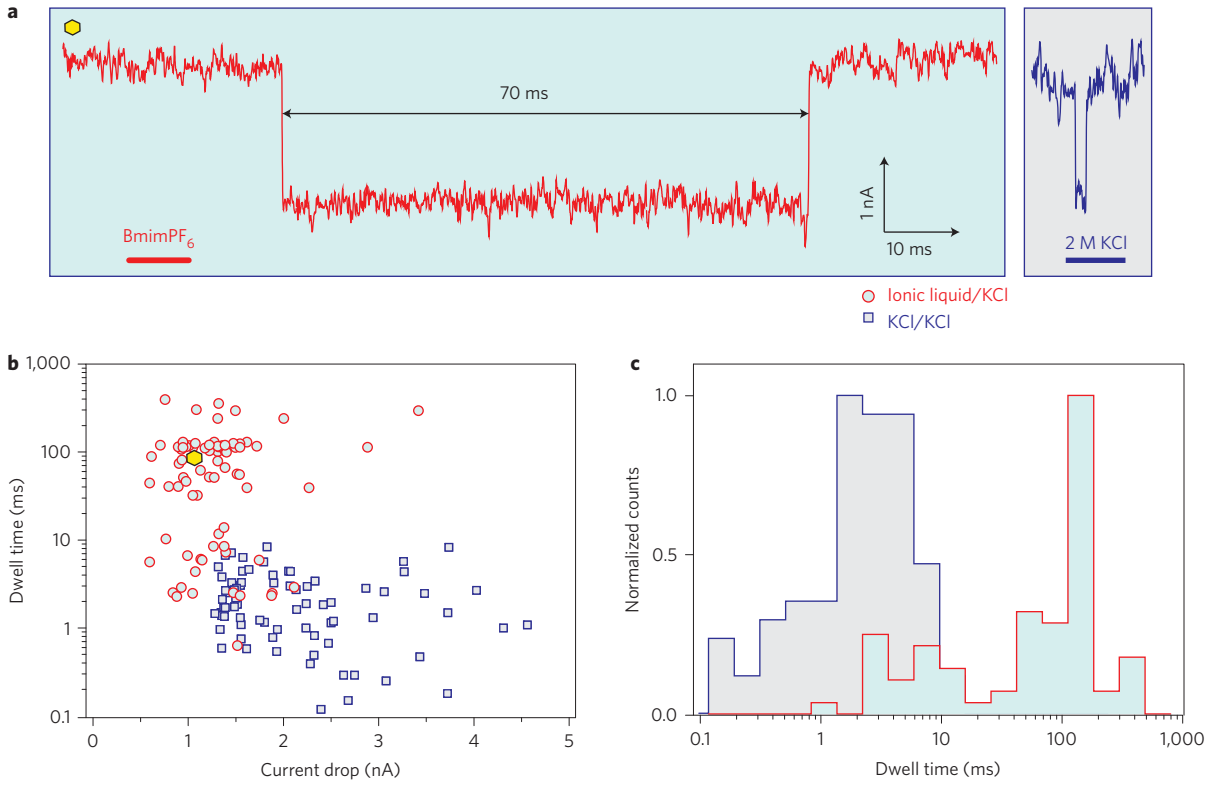

Figure 2 | Slowing of DNA translocation. a, Example of a 48.5 kbp λ-dsDNA translocation event in a viscosity gradient system. The corresponding current drop represents a single DNA molecule passing through a MoS_2 pore with a diameter of 20 nm. Right: a typical translocation trace for 48.5 kbp λ-dsDNA obtained using the same nanopore in the absence of the viscosity gradient, resulting in translocation times that are two orders of magnitude shorter. The displayed traces are downsampled to 10 kHz. **b**, Scatter plots for dwell time versus current signal of λ-dsDNA translocation in water (blue squares) and in our viscosity gradient system (red circles) obtained using the same 20-nm-diameter MoS_2 nanopore. Yellow hexagon: position of the event shown in **a**. **c**, Histograms of translocation times corresponding to the translocation of λ-dsDNA in water (blue) and the viscosity gradient system (red).

chose 1-butyl-3-methylimidazolium hexafluorophosphate ($BmimPF_6$), because it has a broad viscosity window of 10–400 cP (ref. 26), which can be tuned to optimize the temporal resolution. Tunability can be obtained either by varying the temperature (20–50 °C) or by mixing $BmimPF_6$ and $BmimPF_4$ in different ratios[27]. $BmimPF_6$ is also a friendly solvent for biomolecules and, most importantly, exhibits a good ionic conductivity of 1.4 mS cm^{-1} (ref. 26). It has also been widely used as an electrolyte, with a wide electrochemical window[28]. Previous related attempts to slow DNA translocation speeds used glycerol, which has a low conductivity and limited the approach to a narrow viscosity window (1.2–5 cP)[29]. Consequently, only modest improvements in DNA translocation speed were achieved (3,000 nt ms^{-1})[29].

With our viscosity gradient system, schematically shown in Fig. 1a, it was possible to use pure $BmimPF_6$ without compromising the conductance of the MoS_2 nanopore for all tested nanopore devices. For details of the properties and fabrication of MoS_2 nanopores, see Methods and ref. 18. In pure RTILs, the conductance of even a large nanopore (with a diameter of 17 ± 2 nm) is relatively low (~1 nS)[30] when compared with KCl (conduction of 280 nS in 2 M KCl/2 M KCl) (Fig. 1c). Inspired by the use of concentration gradient systems in nanopores[31], we created a viscosity and concentration gradient system that offers a conductivity of 210 nS. The *cis* chamber in our system contains RTILs ($BmimPF_6$), and the *trans* chamber contains 2 M aqueous KCl solution. It is important to note that we use two types of solvent with completely different physicochemical properties, and in the region inside and close to the pore there is a non-homogeneous phase solution.

To gain insight into the ionic transport through the nanopores in the presence of an inhomogeneous phase solution, we performed finite element analysis by solving the Poisson–Nernst–Planck (PNP) equation. Figure 1d shows the mass fraction of water molecules, anions and cations as a function of distance from the nanopore at a transmembrane bias voltage of 400 mV. The sub-nanometre membrane thickness ensured that a relatively high number of water molecules diffused from the *trans* into the *cis* chamber. Similarly, anions and cations diffused into their respective chambers. Modelled conductances for 2.5, 5 and 10 nm pores (Supplementary Fig. 1d–f) are in good agreement with our measurements (Supplementary Fig. 1a–c). Interestingly, the mass fraction of water molecules in the *cis* chamber shows only a weak dependence on transmembrane bias, whereas PF_6^- diffusion is strongly affected (Supplementary Fig. 1g).

Slowing down DNA translocation

Having successfully built and characterized the viscosity gradient system, we performed a first translocation experiment by adding 48.5 kbp λ-dsDNA to the *cis* chamber, which was filled with $BmimPF_6$. To minimize the contribution from the nanopore–DNA interaction, which can also significantly slow down DNA translocation[19], we decided to first use MoS_2 nanopores with relatively large diameters (~20 nm, Supplementary Fig. 2a). Figure 2a presents a typical current trace recorded during the translocation of the λ-DNA molecule in the viscosity gradient system with a transmembrane bias voltage of 400 mV. When compared with a typical current trace acquired in a 2 M aqueous KCl solution using the same pore and transmembrane voltage, a temporal improvement is observed, but no reduction in the amplitude of the current drop. Unlike other viscous systems for slowing down DNA translocation, the signal amplitude is preserved due to the conductive

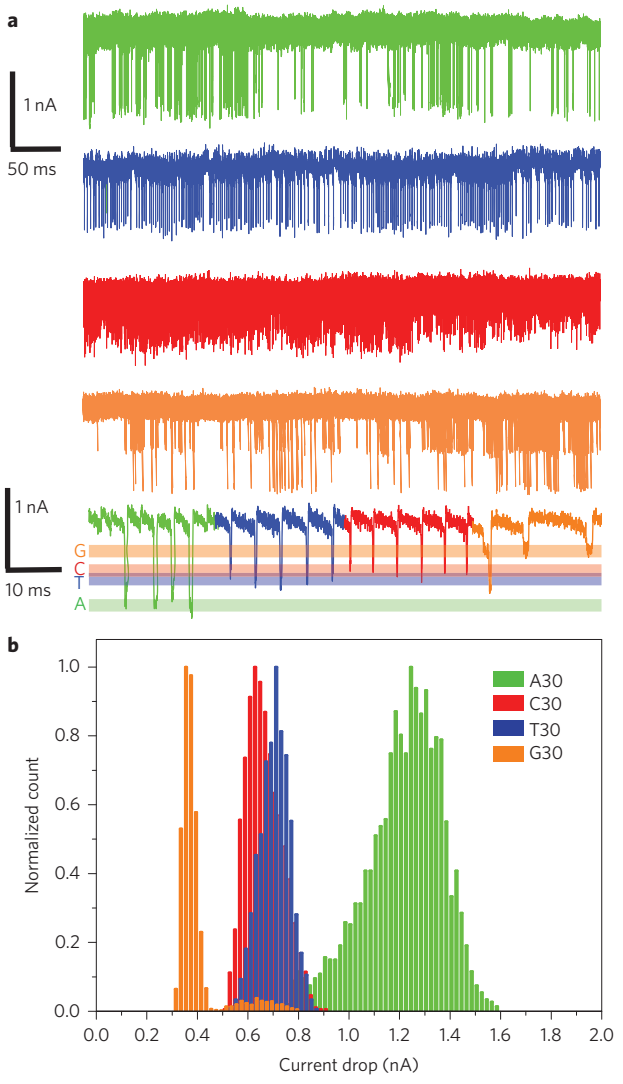

Figure 3 | Differentiation of 30-mer oligonucleotides in the MoS_2 nanopore. a, Translocation signals (0.5 and 0.1 s) for each homopolymer: poly A30 (green), poly C30 (red), poly T30 (blue) and poly G30 (orange). **b**, Normalized histogram of current drops for each DNA homopolymer. Mean values: poly A30, 1.25 ± 0.12 nA; poly C30, 0.64 ± 0.07 nA; poly T30, 0.71 ± 0.06 nA; poly G30, 0.36 ± 0.03 nA. Data were acquired for pure RTIL in the *cis* chamber and 100 mM KCl, 25 mM Tris HCl, pH 7.5, in the *trans* chamber, at +200 mV. Concentration of short DNA homopolymers in RTILs, 0.02 μmol ml^{-1}.

nature of RTILs and the high concentration of chloride ions inside the pore. The average translocation time is 130 ms for λ-DNA in the viscosity gradient system, and 1.4 ms in the 2 M KCl solution, equivalent to two orders of magnitude improvement.

At this point, in the absence of electro-osmotic flow (EOF) and charge reduction for a given pore, DNA molecule and bias voltage, we can introduce the retardation factor r (for details see Supplementary Section 'Theoretical model'). A retardation factor higher than 100 is obtained, which is predominantly due to the increase in viscosity in our viscosity gradient system. However, the scatter plot and DNA translocation histograms in Fig. 2b,c reveal a large spread in dwell times that can be attributed to several factors associated with the viscosity gradient system. In reality, the EOF, charge reduction and long-range hydrodynamic effects, as well as the existence of gradients in the free-energy landscape, have to be included in any model and could result in more complex dynamics of DNA translocation in the viscosity gradient system than assumed in our simplistic model (see Supplementary Information). In addition, it is possible that we have overestimated the value of the viscosity of $BmimPF_6$ in the vicinity of the pore. A more accurate calculation of the retardation factor should include effects related to charge reduction and the presence of the EOF[32]. Due to the negative charges at the surface of the MoS_2 membrane and within the pore, the direction of EOF is opposite to the direction of DNA translocations, and could result in a further slowing down. By comparing the translocation traces before, during and after translocation events, we see that they all have a similar noise level of 520–540 pA (Supplementary Fig. 3). A slight increase in noise is observed during the translocation, which can be explained by the fact that DNA interacts strongly with $BmimPF_6$ via electrostatic interaction between the cationic $Bmim^+$ groups and the DNA phosphates (P–O bonds)[33]. Because of this electrostatic interaction and the hydrophobic association between $Bmim^+$ and bases, DNA molecules can act as carriers for $Bmim^+$ ions from the *cis* to the *trans* chamber.

In general, the single-molecule DNA translocation process can be viewed as a voltage-driven barrier crossing, as shown in Supplementary Fig. 4a. To further explain the retardation mechanism, we explored the voltage dependence of pNEB 193 (a 2,700-bp-long DNA plasmid) translocation dwell times in the MoS_2 nanopore. The observed power law scaling is consistent with Kramer's theory (Supplementary Fig. 4a,b). A free-energy barrier predominately arises from the RTILs and KCl/water interface and includes a change in conformational entropy of the translocating polymer. The threading process across the nanopore in a high-voltage regime follows a force balance model, as described in the Supplementary Information. pNEB is almost 18 times shorter than λ-DNA, but a large retardation is still observed when comparing the average dwell times recorded at 400 mV, under viscosity gradients of 2 ± 0.5 ms and 40 ± 10 μs in a 2 M KCl aqueous solution.

Differentiation of 30-mer DNA homopolymer

To exploit the full potential of our viscosity gradient system, we translocated short homopolymers—$poly(dA)_{30}$, $poly(dT)_{30}$, $poly(dG)_{30}$ and $poly(dC)_{30}$—through a 2.8-nm-diameter pore in single-layer MoS_2 (shown in the TEM micrograph in Supplementary Fig. 2b). DNA–pore interactions can also increase the translocation time by one order of magnitude[34]. This 2.8 nm pore was suspended over a smaller opening in the nitride and, even without any special pretreatment[35], displayed better noise properties than pores suspended over larger openings, showing a current (root mean square) of 59 pA at 0 mV and 89 pA at 200 mV (Supplementary Fig. 7). The noise reduction was achieved by restricting the opening in the freestanding MoS_2 membrane to a hole with a diameter of 100 nm (ref. 36). Self-organization of certain ionic liquids can be further exploited to reduce $1/f$ noise in single nanopores, as shown by Tasserit and co-authors[37]. Figure 3 presents the translocation traces of short DNA homopolymers for periods of 0.5 and 0.1 s, respectively. Four peaks can be clearly distinguished in the histogram of current drops shown in Fig. 3b. The density scatter plots shown in Supplementary Fig. 8a are useful in that they reveal the range of the most probable dwell time for the four types of polynucleotide at the transmembrane bias voltage of 200 mV. The current traces and histogram for the $poly(dG)_{30}$ homopolymer display two peaks. However, from the $poly(dG)_{30}$ density scatter plot (Supplementary Fig. 8) one can easily identify which peak is more probable. Based on the amplitude and temporal signature of the second peak, we believe that it might originate from G-quadruplex formation[38]. Venta and colleagues reported a much faster translocation (20 μs) for such homopolymers using a 1 MHz amplifier in 1.5 nm pores with high applied voltage (1 V)[19]. However, the high-bandwidth amplifier introduced additional noise, and the high voltage might reduce the lifetime of the device. With the present viscosity gradient system and 2.8 nm

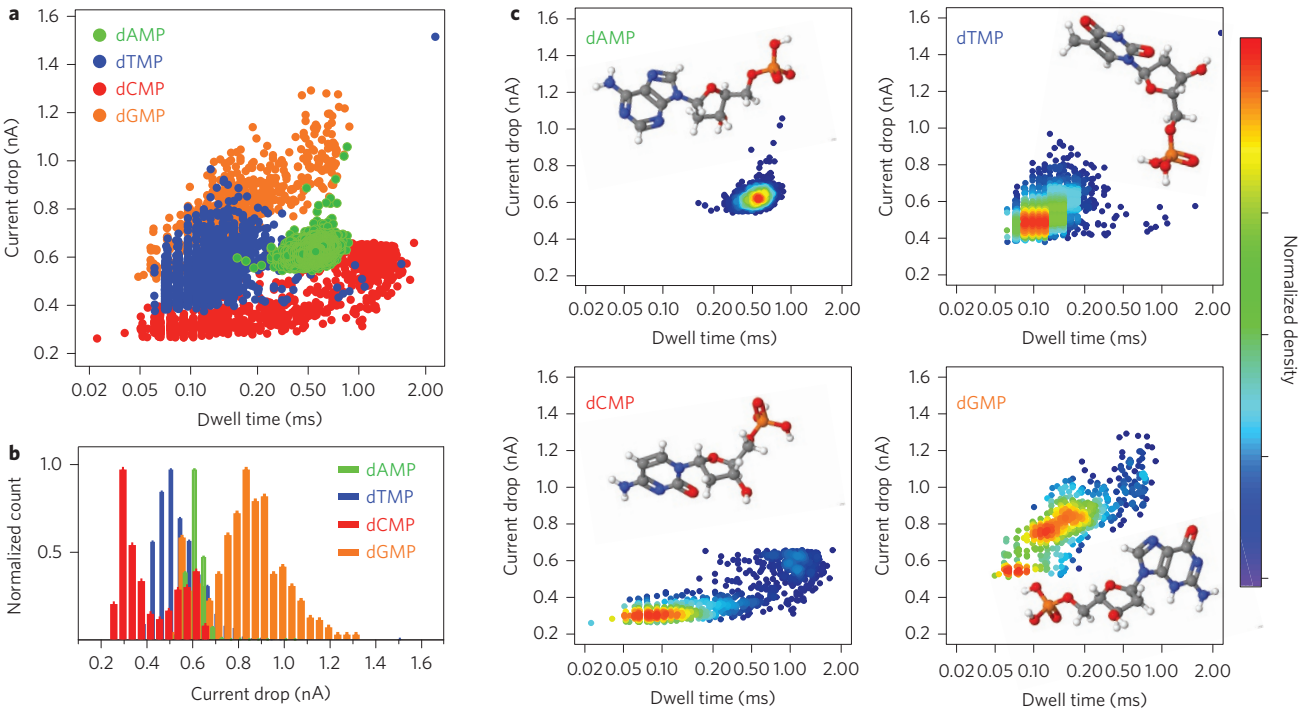

Figure 4 | Identification of single nucleotides in a MoS_2 nanopore. a, Scatter plots of nucleotide translocation events, showing distinguished current drops and dwell times for dAMP, dCMP, dTMP and dGMP. **b**, Normalized histogram of current drops for dAMP, dTMP, dCMP and dGMP. **c**, Density plots of single nucleotides in the MoS_2 nanopore. Positions of the hot spot: dAMP (0.5, 0.62); dTMP (0.09, 0.49); dCMP (0.06. 0.31); dGMP (0.15, 0.83). Right: colour map showing the normalized density distribution of events. Data were acquired with pure RTIL in the *cis* chamber and 100 mM KCl, 25 mM Tris HCl, pH 7.5, in the *trans* chamber, at +200 mV. Nucleotide concentration in RTILs, 5 μg ml^{-1}. Insets: Three-dimensional models of nucleotide chemical structures.

pore, we achieved 10–50 times slowing compared with the results of Venta and co-workers[19].

Identification of single nucleotides

Finally, using the same 2.8-nm-diameter MoS_2 nanopore, we translocated the single nucleotides dAMP, dTMP, dGMP and dCMP. The exceptional durability of the MoS_2 nanopore allowed us to perform eight consecutive experiments with high throughput (more than 10,000 events were collected, enabling robust statistical analysis; Figs 3 and 4) in the same pore. Each experiment was preceded by flushing of the fluidics and by a short control experiment to confirm the absence of the analyte from the previous experiment. Not only does this show the extraordinary resilience of our nanopores, but, to our surprise, the dwell times of single nucleotides are comparable to those of 30-mer homopolymers. At this scale, when comparing the dwell times of single nucleotides with homopolymers, one needs to account for the charge reduction difference that will result in a lower net force acting on the single nucleotide than on the homopolymers. In pores with diameters of <5 nm, the observed translocation retardation is a cumulative effect that has several components: interaction of the translocating molecule with the pore wall, an electrostatic interaction between the $Bmim^+$ cations and the phosphate groups of DNA, the hydrophobic association between the $Bmim^+$ and DNA bases[39] and, finally, the viscosity gradient. The contribution of the viscosity gradient to the retardation will increase with increasing DNA length. Consequently, for single nucleotides this contribution is decreased, but, due to the charge reduction, the lower net force acting on the single nucleotide might account for the observed long translocation times of these single nucleotides.

The use of single-layer MoS_2 as the membrane material and the viscosity gradient system in combination with the small nanopore have been crucial for the single nucleotide discrimination shown in Fig. 4. Supplementary Fig. 9 presents translocation traces for four single nucleotides for periods of 0.5 and 0.1 s. Here, the obtained translocation speed is in the range 1–50 nt ms^{-1}. In accordance with the physical dimensions for four nucleotides, we observe a largest current drop for dGMP, centred at 0.8 nA and a smallest current drop for the smallest single nucleotide dCMP, centred at 0.3 nA. These observations are in good agreement with the results obtained for single nucleotide discrimination using protein pores[1–3]. Although the current drop for dAMP is slightly larger than that for dTMP (0.65 nA, compared with 0.45 nA), we believe that this inconsistency might be due to the stronger $Bmim^+$ affinity towards dAMP compared with dTMP[40]. It has been established that RTILs can selectively bind to DNA[33], and that RTILs based on metal chelate anions could be designed to have specific bonding to the bases[41]. In our system, this could be further exploited to amplify the small differences between the bases. Using the ionic current drops of only 500–3,000 events for four nucleotides, we performed a Welch's *t*-test and found that all *P*-values were less than 0.0001. Moreover, this simple statistical analysis revealed the minimum event number to be 6–9 for nucleotide identification with a confidence of 99%. With the addition of other parameters such as dwell time it might be possible to identify single nucleotides with just one read, while the presence of the direct bandgap in MoS_2 should allow for straightforward multiplexing in a detection scheme based on the transverse current. We also reproduced the discrimination of single nucleotides in a slightly bigger pore (diameter of 3.3 nm) under the same conditions of the viscosity gradient system (Supplementary Fig. 10) and with a similar number of events (>10,000).

On translocating single nucleotides (such as dAMP) and increasing the potential from 200 to 400 mV, we observed increases in the

current drop amplitudes (Supplementary Fig. 11), further confirming that the observed events are indeed from single nucleotide translocation. However, applying a higher potential caused an increase in noise. The data presented in Supplementary Figs 10 and 12 were therefore collected at 200 mV. As expected, in the 3.3 nm pore, the translocation events (>10,000) were faster and produced smaller current amplitude drops than in the 2.8 nm pore and other smaller pores (Supplementary Fig. 12). However, the trend of current drops for different types of nucleotide remained the same, as shown in Fig. 4 (dGMP > dAMP > dTMP > dCMP). As for the 2.8 nm pore, on performing the Welch's *t*-test, we found that 14 events were needed for nucleotide identification with 99% confidence. Supplementary Fig. 12 shows the correlation between mean current drops related to four nucleotides and pore sizes. The dashed line between 3.5 and 4 nm indicates the maximum pore size that still allows nucleotide differentiation. Translocating nucleotides in pores as small as 2 ± 0.2 nm can dramatically increase the signal-to-noise ratio up to 16.

To conclude, we have demonstrated that single-nucleotide identification can be achieved in MoS_2 nanopores by using a viscosity gradient to regulate the translocation speed. The viscosity gradient system can not only be used in standard ionic sensing experiments, but can be potentially combined with other schemes of nanopore sensing such as transverse current signal detection. The ultrahigh viscosity of ionic liquids results in reduced capture rates. Therefore, an optimal experimental configuration would capitalize on high-end electronics[19] and the viscosity gradient system presented here with a suitable capture rate. We believe that combining ionic liquids and monolayer MoS_2 nanopores, together with the readout of transverse current either using the tunnelling[42,43] or FET modality[4,23], would meet all the necessary requirements for DNA strand-sequencing such as optimal time resolution and signal resolution. This could also be achieved in a platform that allows multiplexing, thereby reducing costs and enhancing signal statistics.

Methods

Methods and any associated references are available in the online version of the paper.

Received 27 May 2014; accepted 20 August 2015; published online 21 September 2015

References

1. Astier, Y., Braha, O. & Bayley, H. Toward single molecule DNA sequencing: direct identification of ribonucleoside and deoxyribonucleoside 5′-monophosphates by using an engineered protein nanopore equipped with a molecular adapter. *J. Am. Chem. Soc.* **128,** 1705–1710 (2006).
2. Clarke, J. *et al.* Continuous base identification for single-molecule nanopore DNA sequencing. *Nature Nanotech.* **4,** 265–270 (2009).
3. Laszlo, A. H. *et al.* Decoding long nanopore sequencing reads of natural DNA. *Nature Biotechnol.* **32,** 829–833 (2014).
4. Traversi, F. *et al.* Detecting the translocation of DNA through a nanopore using graphene nanoribbons. *Nature Nanotech.* **8,** 939–945 (2013).
5. Feng, J. *et al.* Electrochemical reaction in single layer MoS_2: nanopores opened atom by atom. *Nano Lett.* **15,** 3431 (2015).
6. Kasianowicz, J. J., Brandin, E., Branton, D. & Deamer, D. W. Characterization of individual polynucleotide molecules using a membrane channel. *Proc. Natl Acad. Sci. USA* **93,** 13770–13773 (1996).
7. Carson, S. & Wanunu, M. Challenges in DNA motion control and sequence readout using nanopore devices. *Nanotechnology* **26,** 074004 (2015).
8. Venkatesan, B. M. & Bashir, R. Nanopore sensors for nucleic acid analysis. *Nature Nanotech.* **6,** 615–624 (2011).
9. Branton, D. *et al.* The potential and challenges of nanopore sequencing. *Nature Biotechnol.* **26,** 1146–1153 (2008).
10. Garaj, S. *et al.* Graphene as a subnanometre trans-electrode membrane. *Nature* **467,** 190–193 (2010).
11. Merchant, C. A. *et al.* DNA translocation through graphene nanopores. *Nano Lett.* **10,** 2915–2921 (2010).
12. Schneider, G. F. *et al.* DNA translocation through graphene nanopores. *Nano Lett.* **10,** 3163–3167 (2010).
13. Wells, D. B., Belkin, M., Comer, J. & Aksimentiev, A. Assessing graphene nanopores for sequencing DNA. *Nano Lett.* **12,** 4117–4123 (2012).
14. Lv, W. P., Chen, M. D. & Wu, R. A. The impact of the number of layers of a graphene nanopore on DNA translocation. *Soft Matter* **9,** 960–966 (2013).
15. Husale, S. *et al.* ssDNA binding reveals the atomic structure of graphene. *Langmuir* **26,** 18078–18082 (2010).
16. Schneider, G. F. *et al.* Tailoring the hydrophobicity of graphene for its use as nanopores for DNA translocation. *Nature Commun.* **4,** 2619 (2013).
17. Zhou, Z. *et al.* DNA translocation through hydrophilic nanopore in hexagonal boron nitride. *Sci. Rep.* **3,** 3287 (2013).
18. Liu, K., Feng, J., Kis, A. & Radenovic, A. Atomically thin molybdenum disulfide nanopores with high sensitivity for DNA translocation. *ACS Nano* **8,** 2504–2511 (2014).
19. Venta, K. *et al.* Differentiation of short, single-stranded DNA homopolymers in solid-state nanopores. *ACS Nano* **7,** 4629–4636 (2013).
20. Larkin, J. *et al.* Slow DNA transport through nanopores in hafnium oxide membranes. *ACS Nano* **7,** 10121–10128 (2013).
21. Liu, X. *et al.* Top-down fabrication of sub-nanometre semiconducting nanoribbons derived from molybdenum disulfide sheets. *Nature Commun.* **4,** 1776 (2013).
22. Radisavljevic, B., Radenovic, A., Brivio, J., Giacometti, V. & Kis, A. Single-layer MoS_2 transistors. *Nature Nanotech.* **6,** 147–150 (2011).
23. Xie, P., Xiong, Q. H., Fang, Y., Qing, Q. & Lieber, C. M. Local electrical potential detection of DNA by nanowire–nanopore sensors. *Nature Nanotech.* **7,** 119–125 (2012).
24. Farimani, A., Min, K. & Aluru, N. DNA base detection using a single-layer MoS_2. *ACS Nano* **8,** 7914 (2014).
25. Keskin, S., Kayrak-Talay, D., Akman, U. & Hortacsu, O. A review of ionic liquids towards supercritical fluid applications. *J. Supercrit. Fluids* **43,** 150–180 (2007).
26. Carda-Broch, S., Berthod, A. & Armstrong, D. W. Solvent properties of the 1-butyl-3-methylimidazolium hexafluorophosphate ionic liquid. *Anal. Bioanal. Chem.* **375,** 191–199 (2003).
27. Khupse, N. D., Kurolikar, S. R. & Kumar, A. Temperature dependent viscosity of mixtures of ionic liquids at different compositions. *Indian J. Chem. A* **49,** 727–730 (2010).
28. Joshi, M. D. & Anderson, J. L. Recent advances of ionic liquids in separation science and mass spectrometry. *RSC Adv.* **2,** 5470–5484 (2012).
29. Fologea, D., Uplinger, J., Thomas, B., McNabb, D. S. & Li, J. L. Slowing DNA translocation in a solid-state nanopore. *Nano Lett.* **5,** 1734–1737 (2005).
30. Davenport, M., Rodriguez, A., Shea, K. J. & Siwy, Z. S. Squeezing ionic liquids through nanopores. *Nano Lett.* **9,** 2125–2128 (2009).
31. Wanunu, M., Morrison, W., Rabin, Y., Grosberg, A. Y. & Meller, A. Electrostatic focusing of unlabelled DNA into nanoscale pores using a salt gradient. *Nature Nanotech.* **5,** 160–165 (2010).
32. Yusko, E. C., An, R. & Mayer, M. Electroosmotic flow can generate ion current rectification in nano- and micropores. *ACS Nano* **4,** 477–487 (2010).
33. Chandran, A., Ghoshdastidar, D. & Senapati, S. Groove binding mechanism of ionic liquids: a key factor in long-term stability of DNA in hydrated ionic liquids? *J. Am. Chem. Soc.* **134,** 20330–20339 (2012).
34. Wanunu, M., Sutin, J., McNally, B., Chow, A. & Meller, A. DNA translocation governed by interactions with solid-state nanopores. *Biophys. J.* **95,** 4716–4725 (2008).
35. Tabard-Cossa, V., Trivedi, D., Wiggin, M., Jetha, N. N. & Marziali, A. Noise analysis and reduction in solid-state nanopores. *Nanotechnology* **18,** 305505 (2007).
36. Garaj, S., Liu, S., Golovchenko, J. A. & Branton, D. Molecule-hugging graphene nanopores. *Proc. Natl Acad. Sci. USA* **110,** 12192–12196 (2013).
37. Tasserit, C., Koutsioubas, A., Lairez, D., Zalczer, G. & Clochard, M. Pink noise of ionic conductance through single artificial nanopores revisited. *Phys. Rev. Lett.* **105,** 260602 (2010).
38. Simonsson, T. G-quadruplex DNA structures—variations on a theme. *Biol. Chem.* **382,** 621–628 (2001).
39. Ding, Y. H., Zhang, L., Xie, J. & Guo, R. Binding characteristics and molecular mechanism of interaction between ionic liquid and DNA. *J. Phys. Chem. B* **114,** 2033–2043 (2010).
40. Cardoso, L. & Micaelo, N. M. DNA molecular solvation in neat ionic liquids. *ChemPhysChem* **12,** 275–277 (2011).
41. Zhang, P. F. *et al.* Ionic liquids with metal chelate anions. *Chem. Commun.* **48,** 2334–2336 (2012).
42. Lagerqvist, J., Zwolak, M. & Di Ventra, M. Fast DNA sequencing via transverse electronic transport. *Nano Lett.* **6,** 779–782 (2006).
43. Ohshiro, T. *et al.* Single-molecule electrical random resequencing of DNA and RNA. *Sci. Rep.* **2,** 501 (2012).

Acknowledgements

The authors thank J. Wu and H. Zhang for discussions about the physicochemical characteristics of ionic liquids and P. De los Rios for discussion about the force drag

mechanism. The authors acknowledge the Centre Interdisciplinaire de Microscopie Electronique (CIME) at EPFL for access to electron microscopes, and special thanks go to D.T.L. Alexander for providing training and technical assistance with the TEM. Device fabrication was partially carried out at the EPFL Center for Micro/Nanotechnology (CMi). The authors thank all members from LBEN and LANES for assistance and discussions. The work was supported financially by the European Research Council (grant no. 259398, PorABEL: Nanopore integrated nanoelectrodes for biomolecular manipulation and sensing, and SNF Sinergia grant no. 147607). The authors thank C. Dekker for reading the manuscript.

Author contributions

J.F. and A.R. conceived the idea. J.F., K.L. and A.R designed the experiments. J.F. and K.L. fabricated and characterized the devices, performed experiments and analysed the data. R.D.B. performed single-molecule fluorescence measurements. S.K and R.D.B. performed COMSOL modelling. D.D. performed chemical vapour deposition MoS_2 growth with A.K.'s supervision. J.F., K.L., A.K. and A.R. wrote the paper. All authors provided important suggestions for the experiments, discussed the results and contributed to the manuscript.

Additional information

Supplementary information is available in the online version of the paper. Reprints and permissions information is available online at www.nature.com/reprints. Correspondence and requests for materials should be addressed to A.R.

Competing financial interests

The authors declare an intellectual property interest in a provisional patent WO/121394 A1.

Methods

The devices were fabricated using a previously published procedure[18]. Briefly, exfoliated or chemical vapour deposition-grown thin layers of MoS_2 were transferred either from SiO_2 or sapphire substrates and suspended on SiN_x membranes. Nanopores were drilled using a JEOL 2200FS high-resolution transmission electron microscope, as described by Liu and co-authors[18]. The chips with nanopores were sealed using silicone O-rings between two polymethylmethacrylate chambers as reservoirs. After mounting, the entire flow cell was flushed with H_2O:ethanol solution (1:1, vol:vol) and wetted for at least 30 min. This was followed by the injection of 2 M KCl solution buffered with 10 mM Tris-HCl and 1 mM EDTA at pH 7.0 and $BmimPF_6$ (Sigma Aldrich) to perform current–voltage (I–V) characteristics measurements. A pair of chlorinated Ag/AgCl electrodes were immersed in two reservoirs and connected to an Axopatch 200B patch clamp amplifier (Molecular Devices), which was used to measure the ionic current as a function of time. Before starting experiments, the current offset was adjusted at zero bias. The device was run at the applied voltage for at least 1 h to perform blank experiments. DNA samples were diluted in pure $BmimPF_6$ by mixing 10 µl λ-DNA stock solution with $BmimPF_6$. DNA samples (pNEB193, plasmid 2.7 kbp, New England; λ-DNA, 48 kbp, New England) were purchased from a commercial supplier, aliquoted, and stored at −20 °C before use. Short homopolymers (Microsynth) and nucleotides (Sigma Aldrich) were purchased in dry form and directly dissolved in RTIL. An NI PXI-4461 card was used for data digitalization and custom-made LabView software for data acquisition. The sampling rate was 100 kHz, and a built-in low-pass filter at 10 kHz was used. Data analysis enabling event detection was performed offline using a custom open source Matlab code, OpenNanopore[44] (http://lben.epfl.ch/page-79460-en.html). The baseline was recalculated using an average of 100 points before the start of each event. The same criteria were used for all compared data. The CUSUM algorithm was used to fit the levels inside every event. The current drop was then calculated by subtracting the corresponding averaged baseline from each level. Each type of DNA and single nucleotide was translocated in at least two different devices, and representative and reproducible results and analyses are presented.

References

44. Raillon, C., Granjon, P., Graf, M., Steinbock, L. J. & Radenovic, A. Fast and automatic processing of multi-level events in nanopore translocation experiments. *Nanoscale* **4,** 4916–4924 (2012).